# X-ray fluorescence imaging of uranium distribution in human dopaminergic cells

Asuncion Carmona, Andrea Somogyi, Stephane Roudeau, Francesco Porcaro, Kadda Medjoubi, Claude Vidaud, Veronique Malard, Carole Bresson, Richard Ortega

# X-Ray Fluorescence Imaging of Uranium Distribution in Human Dopaminergic Cells

Asuncion Carmona[1, a)], Andrea Somogyi[2], Stephane Roudeau[1], Francesco Porcaro[1], Kadda Medjoubi[2], Claude Vidaud[3], Veronique Malard[4], Carole Bresson[5], and Richard Ortega[1]

[1]*Univ. Bordeaux, CNRS, LP2i Bordeaux, UMR 5797, F-33170 Gradignan, France*
[2]*Nanoscopium, Synchrotron SOLEIL, F-91190 Saint-Aubin, France*
[3]*CEA, BIAM, Institut de Biosciences et Biotechnologies d'Aix-Marseille, F-30207 Bagnols Sur Ceze, France*
[4]*Aix Marseille Univ, CEA, CNRS, BIAM, IPM, F-13108 Saint Paul-Lez-Durance, France*
[4]*Univ. Paris-Saclay, CEA, Service d'Etudes Analytiques et de Reactivite des Surfaces, F-91191 Gif-sur-Yvette, France*

[a)]Corresponding author: asuncion.carmona@u-bordeaux.fr

**Abstract.** Uranium exposure can cause neurological disorders, even at low non-cytotoxic concentrations, especially towards the dopaminergic pathway. To date, the mechanisms of uranium neurotoxicity are still poorly understood. One way to deepen the understanding of uranium neurotoxicity is to determine its localization within neurons. However, mapping low concentrations of uranium in subcellular areas is challenging. We have overcome this analytical challenge by using the capabilities of Nanoscopium beamline at SOLEIL synchrotron. The beam, of 17.6 keV energy, was focused with a Kirkpatrick-Baez mirror-pair, providing a spatial resolution in both directions of 300 nm and keeping an incident flux of $10^{10}$ photon/s. Between 2 to 4 hours were required to image a single cell, maintaining a pixel size of 300 nm and a dwell time of 300 ms per pixel. The analyses were conducted at room temperature, under atmospheric conditions, and using two silicon drift detectors located at 120° with respect to the beam direction on both sides of the sample. Human dopaminergic SH-SY5Y cells were differentiated into mature neurons and continuously exposed for seven days to a non-cytotoxic concentration of 10 μM of natural uranium, under the uranyl-carbonato soluble form. Living cells were transfected with transitory commercial kits to express fluorescently-labeled proteins of interest. We observed by epi-fluorescence microscopy the localization of lysosomes, early/late endosomes, nucleus and fetuin-A, a protein known for its high affinity for uranium. Epi-fluorescence microscopy was performed in living cells and the samples were cryofixed immediately after, by plunge freezing in isopentane cooled with liquid nitrogen, and further freeze-dried. Synchrotron x-ray fluorescence imaging (SXRF) revealed the formation of submicron-sized uranium aggregates in the cytoplasm. Some uranium aggregates were colocalized with iron hot-spots, suggesting common metabolic storage pathways. A strict correlation between the distribution of uranium and fluorescently- labeled fetuin-A could not be evidenced. The intracellular distribution of uranium followed a similar localization pattern than lysosomes and late endosomes, characterized by an accumulation on the same regions of the cell and similar grain size distribution. We evaluated the size of these uranium-rich areas and found that their diameter could range from <300 nm to 1.5 μm. The uranium aggregates contained neither calcium nor phosphorus, indicating that detoxification mechanisms differ from those described in bone or kidney cells, which involve the precipitation of calcium phosphate. Thanks to the quantification capability of SXRF imaging, we calculated that cytoplasmic uranium aggregates accounted on average for 62% of the total intracellular uranium. We suggest that the remaining soluble uranium fraction would be responsible for most of the toxicity. In conclusion, our results indicate that cytoplasmic uranium aggregation could be a mechanism of neuronal defense through the sequestration of uranium into less toxic species.

# INTRODUCTION

Uranium is a natural weakly radioactive element with adverse health effects mainly due to its chemical rather than radiological toxicity[1]. In case of high uranium exposure, the main targets of uranium toxicity in human are the kidneys and the bones where it accumulates for years. Less severe effects are however observed on the liver, lungs, reproductive and nervous systems[1]. Uranium exposure induces neurobehavioral changes such as increased locomotor activity, perturbation of the sleep-wake cycle, decreased memory, and increased anxiety on animal models. The mechanisms by which uranium induces neurological alterations are not fully known. The dopaminergic transmission system represents one of the main targets of uranium chemical neurotoxicity[2].

The aim of this study was to provide some understanding on the mechanisms of uranium disruption of the dopaminergic system, by the investigation of uranium distribution in human dopaminergic cells. We previously addressed the question of uranium intracellular distribution using micro-PIXE (Particle Induced X-ray Emission) imaging, a technique applied with a spatial resolution of 2 µm and a limit of detection of about 10 $\mu g.g^{-1}$ for uranium imaging. Micro-PIXE imaging revealed the uranium localization in cytoplasmic regions of SHSY5Y dopaminergic cells, particularly observable after continuous exposure to sub-cytotoxic (125 µM) and slightly toxic (250 µM) uranyl concentrations[3]. The nature of these uranium-rich cytoplasmic regions and their existence for lower concentration exposures have yet to be determined.

In the present study, we successfully performed Synchrotron x-ray fluorescence imaging (SXRF) at SOLEIL Nanoscopium beamline with a spatial resolution of 300 nm, a detection limit in the 0.1-1 $\mu g.g^{-1}$ range, on SH-SY5Y dopaminergic cells exposed to 10 µM uranium, a concentration far from the cytotoxicity threshold to mimic neurotoxic but not cytotoxic exposures. We applied a protocol for correlative light/SXRF microscopy[4]. Such method allowed to image intracellular uranium distribution and to check for the presence, or not, of uranium in specific cellular compartments by comparing and correlating the optical fluorescence images of marked organelles in live cells with SXRF elemental maps[5].

# MATERIAL AND METHODS

## Sample preparation

SH-SY5Y neuroblastoma cells were used as a model of dopaminergic neurons after terminal differentiation[3, 5]. Sample holders for SXRF consisted in a thin (2 µm) ultrapure polycarbonate film stretched over a polyether ether ketone (PEEK) frame with a 5 mm x 5 mm window where cells are grown[6]. Sample holders were sterilized in analytical grade ethanol, rinsed with ultrapure water and dried in sterile conditions. To enhance cell attachment, polycarbonate films were coated with a solution of 0.01 $mg.mL^{-1}$ of bovine serum albumin, 0.01 $mg.mL^{-1}$ of human fibronectin, and 0.03 $mg.mL^{-1}$ of collagen type I (all products from Sigma-Aldrich). SH-SY5Y cells were seeded onto each SXRF sample holder at 25,000 $cells.cm^{-2}$. Cells were thereafter grown on polycarbonate films, differentiated with retinoic acid and 12-O-tetradecanoylphorbol-13-acetate during 7 days.

Early, late endosome and lysosome cellular organelles were labeled on living cells by means of the CellLight™ transitory transfection kits (ThermoFisher). Then cells were exposed to 10 µM natural uranyl, under the uranyl-carbonato soluble form, for 7 days. Cell exposure to fluorescently labeled Alexa Fluor® 488 fetuin-A was carried out after uranium exposure. Live cell imaging of the fluorescent labels was recorded with an epifluorescence microscope (Olympus BX51). Immediately after live cell microscopy, cells were rinsed with a 150 mM ammonium acetate buffer solution, pH 7.4, prepared in ultrapure water (Fisher) to remove traces of extracellular elements. Then cells were cryofixed by rapid plunge freezing in isopentane chilled with liquid nitrogen down to -160°C, and freeze-dried at -90°C under primary vacuum (Christ Alpha 1-4 freeze-drier).

## SXRF imaging

SXRF analyses were carried out at Nanoscopium beamline from the French national facility, synchrotron SOLEIL[7]. SXRF element distributions were acquired by using a 17.6 keV X-ray beam just above the L3 absorption edge of uranium. The incoming X-ray beam was focused to 300 x 300 $nm^2$ size with a Kirkpatrick-Baez nano-focusing mirror-pair, resulting in about $10^{10}$ $ph.s^{-1}$ flux. In order to map the uranium distributions in single cells, around 2-4 hours per cell was required with 300 ms dwell time per pixel and 300 nm pixel size. A home-made MATLAB code was used for on-line data treatment at the Nanoscopium beamline for extracting the corrected elemental distribution maps from the identified X-ray region of interests. 3D XRF data cubes were also extracted by the MATLAB code for further data-processing by PyMca software[8].

## RESULTS

The excellent sensitivity and spatial resolution of the SXRF technique enabled to investigate uranium subcellular distribution in dopaminergic cells exposed to 10 µM uranium, a concentration far from the cytotoxicity threshold but showing already neurotoxic effects such as the alteration of the monoaminergic pathway[3]. SXRF revealed the formation of submicron uranium aggregates in the cytoplasm (Figure 1), which had not been observed previously with other techniques. Thanks to the quantification capability of SXRF imaging, we calculated that cytoplasmic uranium aggregates accounted on average for 62% of the total intracellular uranium[4]. Some uranium aggregates were colocalized with iron hot-spots, suggesting common metabolic storage pathways[4]. The exact nature of these uranium aggregates and their mechanism of formation in SH-SY5Y cells remains elusive. Contrary to what has been described for exposure conditions et higher concentrations, and in other cell types, phosphorus or calcium were not detected in the submicron uranium aggregates. The mechanism of cytoplasmic aggregation of uranium in neuron-like cells is thus probably different from the mechanisms described in osteoblasts, which involve precipitation of calcium phosphate by biomineralization pathways[9], or in macrophages, which result in precipitation of uranium in lysosomes because of the specific activity of the lysosomal acid phosphatase in these cells[10].

We also explored other hypotheses to identify the nature of uranium aggregates by comparing the distribution of uranium with vesicular organelles (lysosomes, early and late endosomes) and with vesicles containing fetuin-A, a protein known for its high affinity for uranium (Figure 1). The intracellular distribution of uranium followed a similar localization pattern than lysosomes and late endosomes, characterized by an accumulation on the same regions of the cell and similar grain size distribution. However, our results do not suggest a strict co-localization of uranium with the endo-lysosomal pathway or with vesicles containing labeled fetuin-A. We evaluated the size of these uranium-rich areas and found that their diameter could range from <300 nm to 1.5 µm. Therefore, considering the size of the uranium aggregates, the fact that they are not co-localized with phosphorous or calcium, and that they are not strictly co-localized with the endo-lysosomal and fetuin-A vesicles, it is likely that uranium aggregates could be formed directly within the cytosol of SH-SY5Y neuron-like cells.

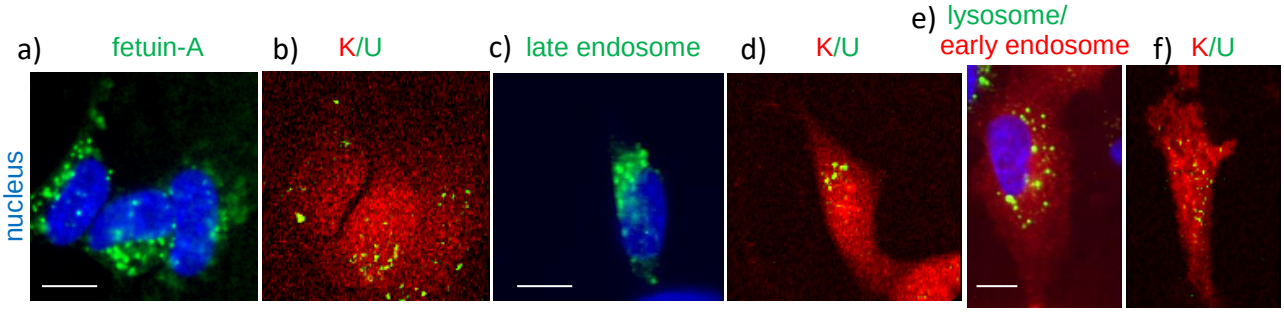


**FIGURE 1.** Uranium distribution in dopamine producing cells and comparison with the localization of fluorescently labeled proteins and organelles. a) Fetuin-A and b) corresponding potassium and uranium distributions. C) Late-endosome and d) corresponding potassium and uranium distributions. e) Lysosome and early endosome and f) corresponding potassium and uranium distributions. Scale bars: 10 µm.

## CONCLUSION

These results suggest that uranium aggregation in SH-SY5Y neuron-like cells may be a cellular defence mechanism against uranium neurotoxicity, which begins at low levels of continuous uranium exposure, resulting in sequestration of uranium into less reactive species (i.e., ferritin binding). How soluble uranium is clustered in uranium-dense cytoplasmic areas will require further research. Clues may come from the coordination chemistry of uranium with biological ligands, with the chemical environment seen by uranium affecting its binding and aggregation. The extent of nonspecific interactions between uranium and proteins is expected to be significant in cells and could lead to the formation of multinuclear uranium clusters with proteins[11]. Multinuclear uranium-protein clusters could represent the initial phase of cytosolic uranium aggregate formation. Although we suggest that this mechanism may be protective, aggregation of uranium with target neurotoxic proteins could contribute to neurotoxicity. Finally, it is important to note that a non-negligible proportion of uranium remains soluble in the cell. This pool of soluble uranium could explain the neurotoxic effects, such as the alteration of dopaminergic metabolism, observed at non-cytotoxic uranyl exposure concentrations.

## ACKNOWLEDGMENTS

This project has received financial support from the CNRS through the MITI interdisciplinary programs, the Nuclear Toxicology program of CEA, and from CNRS-IN2P3.We acknowledge SOLEIL for provision of synchrotron radiation facilities and we would like to thank NANOSCOPIUM staff for assistance in using the beamline. The authors are grateful to Dr. Marta Garcia Cortes for the characterization of the Alexa Fluor® 488 labeled fetuin-A solution.

## REFERENCES

1. S. L. Keith, O. M. Faroon, B. A. Fowler, “Uranium”, in *Handbook of the Toxicology of Metals*, (Academic Press, London, 2008) pp. 881-904..
2. C. Dinocourt, M. Legrand, I. Dublineau, P. Lestaevel, Toxicology **337**, 58-71 (2015).
3. A. Carmona, V. Malard, E. Avazeri, S. Roudeau, F. Porcaro, E. Paredes, C. Vidaud, C. Bresson, R. Ortega, NeuroToxicology **68**, 177-188 (2018).
4. S. Roudeau, A. Carmona, L. Perrin, R Ortega, Anal. Bioanal. Chem. **406**, 6979–6991 (2014).
5. A. Carmona, F. Porcaro, A. Somogyi, S. Roudeau, F. Domart, K. Medjoubi, M. Aubert, H. Isnard, A. Nonell, A. Rincel, E. Paredes, C. Vidaud, V. Malard, C. Bresson and R. Ortega, NeuroToxicology **82**, 35–44 (2021).
6. L. Perrin, A. Carmona, S. Roudeau, R. Ortega, J. Anal. Atom. Spectrom. **30**, 2525-2532 (2015).
7. A. Somogyi, K. Medjoubi, G. Baranton, V. Le Roux, M. Ribbens, F. Polack, P. Philippot, J. P. Samama, J. Synchrotron Rad. **22**, 1118–1129 (2015).
8. V. A. Solé, E. Papillon, M. Cotte, P. Walter, J. Susini, Spectrochim. Acta Part B **62**, 63-68 (2007).
9. S. Boonrungsiman, E. Gentleman, R. Carzaniga, N. D. Evans, D. W. McComb, A. E. Porter, M. M. Stevens,. Proc. Natl. Acad. Sci. U. S. A. **109**, 14170-14175 (2012).
10. M.H. Hengé-Napoli, E. Ansoborlo, M. Claraz, J.P. Berry, M.C. Cheynet, Cell. Mol. Biol. **42**, 413-420 (1996).
11. J. D. Van Horn, H., Huang, Coord. Chem. Rev. **250**, 765–775 (2006).